AMERICAN SOCIETY FOR MICROBIOLOGY | Applied and Environmental Microbiology®

BIODEGRADATION

Development of a Targeted Gene Disruption System in the Poly(Ethylene Terephthalate)-Degrading Bacterium *Ideonella sakaiensis* and Its Applications to PETase and MHETase Genes

Shin-ichi Hachisuka,[a] Tarou Nishii,[b] Shosuke Yoshida[a,b]

[a]Institute for Research Initiatives, Division for Research Strategy, Nara Institute of Science and Technology, Ikoma, Nara, Japan
[b]Graduate School of Biological Science, Nara Institute of Science and Technology, Ikoma, Nara, Japan

ABSTRACT Poly(ethylene terephthalate) (PET) is a commonly used synthetic plastic; however, its nonbiodegradability results in a large amount of waste accumulation that has a negative impact on the environment. Recently, a PET-degrading bacterium, *Ideonella sakaiensis* 201-F6 strain, was isolated, and the enzymes involved in PET digestion, PET hydrolase (PETase), and mono(2-hydroxyethyl) terephthalic acid (MHET) hydrolase (MHETase) were identified. Despite the great potentials of *I. sakaiensis* in bioremediation and biorecycling, approaches to studying this bacterium remain limited. In this study, to enable the functional analysis of PETase and MHETase genes *in vivo*, we have developed a gene disruption system in *I. sakaiensis*. The pT18*mobsacB*-based disruption vector harboring directly connected 5′- and 3′-flanking regions of the target gene for homologous recombination was introduced into *I. sakaiensis* cells via conjugation. First, we deleted the orotidine 5′-phosphate decarboxylase gene (*pyrF*) from the genome of the wild-type strain, producing the Δ*pyrF* strain with 5-fluoroorotic acid (5-FOA) resistance. Next, using the Δ*pyrF* strain as a parent strain and *pyrF* as a counterselection marker, we disrupted the genes for PETase and MHETase. The growth of both Δ*petase* and Δ*mhetase* strains on terephthalic acid (TPA; one of the PET hydrolytic products) was comparable to that of the parent strain. However, these mutant strains dramatically decreased the growth level on PET to that on a no-carbon source. Moreover, the Δ*petase* strain completely abolished PET degradation capacity. These results demonstrate that PETase and MHETase are essential for *I. sakaiensis* metabolism of PET.

IMPORTANCE The poly(ethylene terephthalate) (PET)-degrading bacterium *Ideonella sakaiensis* possesses two unique enzymes able to serve in PET hydrolysis. PET hydrolase (PETase) hydrolyzes PET into mono(2-hydroxyethyl) terephthalic acid (MHET), and MHET hydrolase (MHETase) hydrolyzes MHET into terephthalic acid (TPA) and ethylene glycol (EG). These enzymes have attracted global attention, as they have potential to be used for bioconversion of PET. Compared to many *in vitro* studies, including biochemical and crystal structure analyses, few *in vivo* studies have been reported. Here, we developed a targeted gene disruption system in *I. sakaiensis*, which was then applied for constructing Δ*petase* and Δ*mhetase* strains. Growth of these disruptants revealed that PETase is the sole enzyme responsible for PET degradation in *I. sakaiensis*, while PETase and MHETase play essential roles in its PET assimilation.

KEYWORDS poly(ethylene terephthalate) (PET), PET hydrolase (PETase), mono(2-hydroxyethyl) terephthalic acid hydrolase (MHETase), *Ideonella sakaiensis*, genetic manipulation

Environmental pollution caused by plastic waste is currently a focus of global attention. It is estimated that a total of approximately 6,300 million metric tons (Mt) of plastic waste was generated between 1950 and 2015, and approximately 12,000 Mt

Citation Hachisuka S-I, Nishii T, Yoshida S. 2021. Development of a targeted gene disruption system in the poly(ethylene terephthalate)-degrading bacterium *Ideonella sakaiensis* and its applications to PETase and MHETase genes. Appl Environ Microbiol 87:e00020-21. https://doi.org/10.1128/AEM.00020-21.

Editor Isaac Cann, University of Illinois at Urbana-Champaign

Address correspondence to Shosuke Yoshida, ssk-yoshida@bs.naist.jp.

Received 5 January 2021
Accepted 5 July 2021
Accepted manuscript posted online 14 July 2021
Published 26 August 2021

will be discarded in landfills or the natural environment by the end of 2050 if the current use patterns and management trends continue (1). Plastic waste is released into the ocean through multiple paths, including waterways and littering on beaches and coastlines (2, 3), with an estimated 4.8 to 12.7 Mt of plastic waste having entered the ocean from 192 coastal countries in 2010 (2). Furthermore, the components of certain plastic products affect animal health, which raises concerns about their potential risk to human health as well (4, 5).

Poly(ethylene terephthalate) (PET) is a synthetic polymer produced on a large scale and used as raw material for various plastic products, such as bottles and clothes. PET is resistant to degradation in the natural environment, owing to structural elements such as aromatic groups and crystallinity that limit the polymer chain movement along with high surface hydrophobicity (6–8). To date, cascaded recycling that decreases the quality of the polymer material has been developed for PET wastes, which includes a thermomechanical reform, transformation to other applications such as fillers, and an energetic conversion to collect thermal energy as a fuel (9, 10). In contrast, chemical recycling allows the conversion of waste PET into the monomers or oligomers to reconstruct polymers with the same or similar quality. However, this method requires a considerable amount of chemicals in the depolymerization, separation, and purification steps, leading to the production of toxic compounds that cause ecological issues (10). Alternatively, research into enzymatic recycling first demonstrated in 2005 that a polyesterase is capable of hydrolyzing PET (11, 12). Furthermore, a novel bacterium, *Ideonella sakaiensis* 201-F6, capable of degrading PET, was recently isolated (13, 14). *I. sakaiensis* is a Gram-negative, non-spore-forming, aerobic, rod-shaped bacterium belonging to the class *Betaproteobacteria*. The optimal growth conditions have been determined, including the optimal temperature (30 to 37°C) and pH (7 to 7.5), while appropriate culture conditions have also been reported (15). Additionally, a nearly complete genome sequence of this bacterium is available, enabling the prediction of its metabolism (13). *I. sakaiensis* can utilize PET as its primary carbon source, as it produces two enzymes important for hydrolyzing PET. PET hydrolase (PETase; ISF6_4831 protein) hydrolyzes PET into mono(2-hydroxyethyl) terephthalate (MHET), and MHET hydrolase (MHETase; ISF6_0224 protein) hydrolyzes MHET into two monomers, terephthalic acid (TPA) and ethylene glycol (EG).

Thus far, many studies on *I. sakaiensis* enzymes have been carried out, including structural analyses of PETase (16–21) and MHETase (22, 23); enhancement of the PET-hydrolytic activity of PETase by site-directed mutagenesis (8, 18, 20, 21, 24–27); coating the PET film surface with anionic surfactants (28); and heterologous expression and secretion of PETase (29–32). However, no analysis performed has investigated *I. sakaiensis* cells. Lack of gene manipulation systems in this bacterium might deter progress in studies involving *I. sakaiensis*.

This study, therefore, aimed to develop a targeted gene disruption system in *I. sakaiensis* to promote *in vivo* applications, such as gene functional analysis and metabolic engineering. For the exogenous plasmid introduction into *I. sakaiensis* cells, conjugation, a genetic material transfer system via a bridge-like connection between donor and recipient cells (33), was applied. Furthermore, the orotidine 5′-phosphate decarboxylase gene (*pyrF*; involved in the biosynthesis of pyrimidine derivatives such as UMP, UDP, and UTP) was utilized as a selection/counterselection marker. As *pyrF* is involved in the conversion of the pyrimidine analog 5-fluoroorotic acid (5-FOA) into toxic 5-fluorouridine monophosphate, a *pyrF*-deficient mutant exhibits resistance to 5-FOA. Therefore, counterselection based on the expression of *pyrF* in the *pyrF*-deficient mutant is utilized for genome engineering in a wide variety of microorganisms, including *Betaproteobacteria* (34–36). We first introduced a *pyrF* disruption (Δ*pyrF*) vector into the wild-type strain via conjugation and isolated a Δ*pyrF* strain by counterselection with 5-FOA. Further, using the Δ*pyrF* strain as a parent strain and *pyrF* as a selectable marker, we successfully constructed strains with disrupted PETase and MHETase

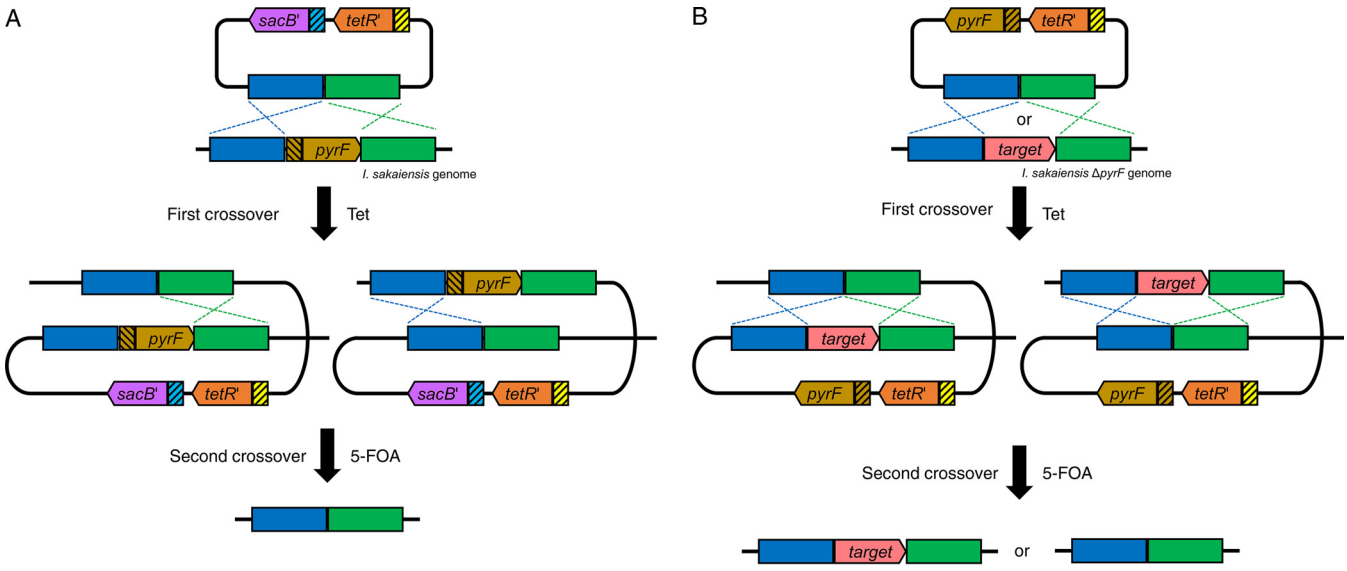

FIG 1 Schematic diagrams of targeted gene disruption by homologous recombination in *I. sakaiensis*. (A) Disruption of *pyrF* and its promoter. The first crossover occurs at either the 5′-flanking region or 3′-flanking region of the target. In the resultant mutants, the second crossover produces the Δ*pyrF* strain (parent strain). (B) Disruption of *petase* and *mhetase*. The first crossover occurs at either 5′-flanking region or 3′-flanking region of the disruption target. The second crossover potentially produces the parent strain or the target gene disruption strain. Yellow and light blue boxes with slant lines indicate the original promoters of *tetR* and *sacB*, respectively, in pT18*mobsacB*. Brown box with slant lines indicates original promoter of *pyrF* in *I. sakaiensis* genome. Blue and green boxes indicate 5′- and 3′-flanking regions of the disruption target, respectively. 5-FOA, 5-fluoroorotic acid; *pyrF*, orotidine 5′-phosphate decarboxylase gene; *sacB*′, levansucrase gene with codon optimization for expression in the genus *Ideonella*; Tet, tetracycline; *tetR*′, tetracycline repressor protein gene with codon optimization for expression in the genus *Ideonella*.

genes (Δ*petase* and Δ*mhetase*). Their growth capacities on TPA, EG, or PET were compared to understand the physiological functions of PETase and MHETase.

RESULTS

Preparation of the *pyrF* disruption strain. We found that *I. sakaiensis* 201-F6 possesses a putative *pyrF* (ISF6_5168 or *pyrF*) on its genome. To utilize the Δ*pyrF* strain as a parent for counterselection using 5-FOA, we aimed to disrupt *pyrF* in *I. sakaiensis*. Considering the relatively high GC content of the *I. sakaiensis* genome (70.4 mol%) (15), marker genes (*tetR* and *sacB*) in the pT18*mobsacB*, a mobilizable vector via conjugation, were replaced with those synthesized with codon optimization suitable for the genus *Ideonella* (see Fig. S1 in the supplemental material), producing pT′18*mobsacB*′ (Fig. S2). Next, DNA fragments of 709 bp (−750 to −42 relative to the *pyrF* initiation) and 770 bp (−20 to +750 relative to the *pyrF* end) were directly connected and inserted into the SmaI site of pT′18*mobsacB*′, resulting in the *pyrF* disruption vector pT′*msB*′D*pyrF*. This vector was designed to eliminate the predicted promoter region of *pyrF* (−41 to −1 relative to the *pyrF* initiation) and to leave the overlap with the neighbor gene (ISF6_5167) (−20 to −1 relative to the *pyrF* end) (Fig. S3).

pT′*msB*′D*pyrF* was introduced into *I. sakaiensis* via conjugation by *Escherichia coli* S17-1. The cells were selected on agar plates containing kanamycin (Kan; for which *E. coli* is sensitive and *I. sakaiensis* is resistant) and tetracycline (Tet; for plasmid integration into the genome [Fig. 1A]). The typical transformation efficiency (the number of transconjugants per donor cell) was approximately 2.5×10^{-5}. Integration of the plasmid into the genome (pop-in) was confirmed by PCR (data not shown). The pop-in strain was then inoculated onto the medium containing 5-FOA to select a strain whose target gene is removed with plasmid pop-out from the genome (pop-out strain). PCR analysis using the primer set designed to anneal outside the regions of homologous recombination (Fig. 2A and B, arrow a) detected a shorter band in the transformant than in the wild-type strain. Another PCR analysis using the primer set designed to anneal within the *pyrF* (Fig. 2A and B, arrow b) detected no band in the transformant, whereas the predicted band was observed in the wild-type strain. These results

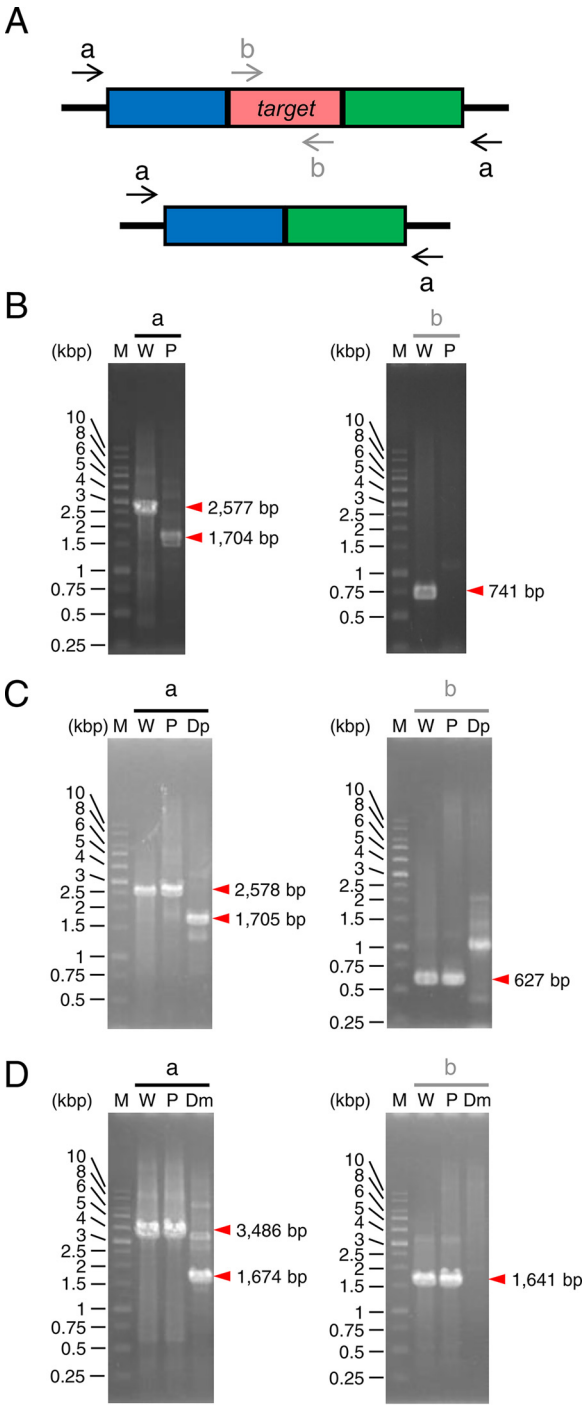

FIG 2 PCR analyses of the gene disruption. (A) DNA primers that anneal to the genome before and after target gene disruption. These primers were used to analyze Δ*pyrF* (B), Δ*petase* (C), and Δ*mhetase* (D) strains. The red box represents the disruption target region. The blue and green boxes represent its 5′- and 3′-flanking regions, respectively. The black arrows (a) and gray arrows (b) denote the primer set designed to anneal outside the target region for homologous recombination and within the target region, respectively. The expected number of base pairs in each DNA fragment is indicated at the right side of the red arrowhead. M, marker; W, wild-type strain; P, parent strain (Δ*pyrF*); Dp, Δ*petase*; Dm, Δ*mhetase*.

demonstrated the transformant is a Δ*pyrF* strain. Here, we tested eight colonies with 5-FOA resistance, all of which showed *pyrF* deletion. This indicates that the homologous recombination occurs at a higher ratio rather than spontaneous loss-of-function mutation(s) into *pyrF* in *I. sakaiensis*.

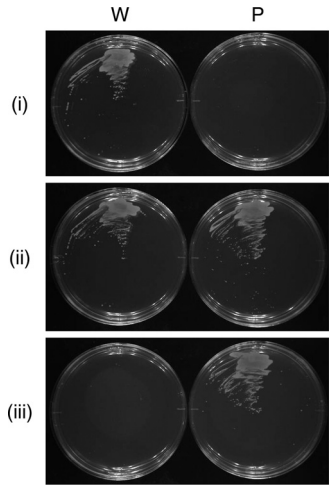

FIG 3 Growth of wild-type (W) and Δ*pyrF* (parent, P) strains. The strains were cultivated on SV agar plates including Mal·H_2O (i), Mal·H_2O-Ura (ii), and Mal·H_2O-Ura-5-FOA·H_2O (iii) at 30°C for 5 days.

sacB, encoding levansucrase, which converts sucrose to levan, a compound toxic to Gram-negative bacteria (37), was utilized as a counterselectable marker (38). To examine whether *sacB*′ functions as a counterselectable marker in *I. sakaiensis*, the pop-in strain (pT′*msB*′D*pyrF*-integrated strain) was cultivated on medium including 5% (wt/vol) sucrose, to which the wild-type strain is resistant. A number of colonies grew; however, *sacB*′ was detected in the 40 colonies examined (data not shown). This shows that *sacB*′ is unlikely to be appropriate as a counterselection marker for *I. sakaiensis*.

Uracil auxotrophy and 5-FOA resistance of the Δ*pyrF* strain. The wild-type strain grew on an SV plate (minimal medium without uracil) containing maltose, whereas the Δ*pyrF* strain displayed no growth on this medium (Fig. 3i). The uracil addition to the medium (final concentration, 10 μg/ml) restored the growth of the Δ*pyrF* strain to a level similar to that of the wild-type strain (Fig. 3ii). Cultivation on an SV plate supplemented with maltose, uracil, and 5-FOA resulted in clear growth of the Δ*pyrF* strain but no growth of the wild-type strain (Fig. 3iii). These results indicate that the Δ*pyrF* strain exhibits uracil auxotrophy and 5-FOA resistance, as expected. Therefore, the Δ*pyrF* strain can be used as a parent strain for *pyrF*-based counterselection using 5-FOA.

Construction of the Δ*petase* and Δ*mhetase* strains. First, to enable the counterselection using 5-FOA in the Δ*pyrF* strain, we replaced *sacB* and its promoter in pT′18*mobsacB* with *I. sakaiensis pyrF* and its promoter, producing pT′18*mobpyrF* (Fig. S2 and S3). Further, the 750-bp upstream/downstream regions of the PETase gene (*petase*) (Fig. S4A) and the 648-bp upstream and 641-bp downstream regions of the MHETase gene (*mhetase*) (Fig. S4B) were inserted into the SmaI site of pT′18*mobpyrF*, resulting in the disruption vectors of *petase* and *mhetase*, pT′*mpF*D*petase* and pT′*mpF*D*mhetase*, respectively.

Figure 1B shows the assumed process of homologous recombination for disrupting target genes using the Δ*pyrF* strain as a parent. Integration of the disruption vectors into the genome of the Δ*pyrF* strain followed by plasmid pop-out from the pop-in strain was carried out with the same procedure as that for Δ*pyrF* strain construction. The pop-out strains potentially include both the parent and disruption strains. Therefore, we performed colony PCR, which identified the disruption strains: 1 of 64 colonies for Δ*petase* and 14 of 32 colonies for Δ*mhetase*. Regarding PCR toward the genomic DNA, when the primer set designed to anneal outside the region for homologous recombination was used, a shorter band was detected in the transformant than in the parent (Fig. 2A, C, and D, arrow a). When the primer set that anneals within *petase* or *mhetase* was used, no specific band was detected in the transformant, whereas a predicted band was detected in the parent (Fig. 2A, C, and D, arrow b). Western blotting with antibodies against PETase and MHETase showed the expression

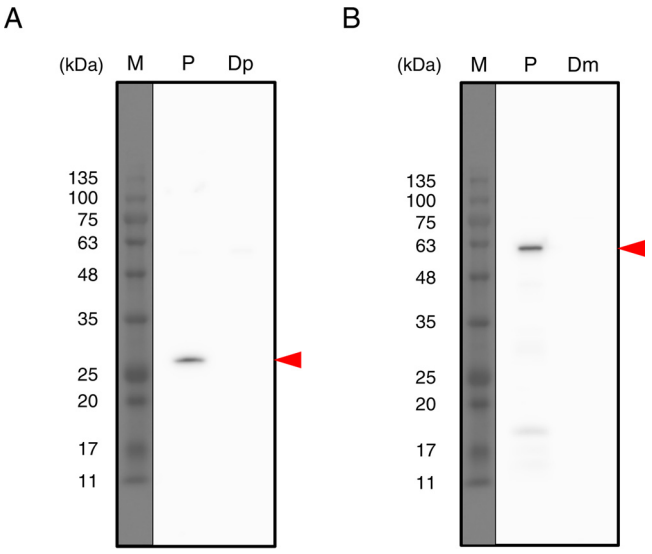

FIG 4 Expression of PETase and MHETase in *I. sakaiensis* strains. The Δ*pyrF*, Δ*petase*, and Δ*mhetase* strains were grown in SV-TPA·2Na and analyzed by Western blotting using polyclonal antibodies against PETase (A) and MHETase (B). Red arrowheads indicate the predicted molecular weight positions of PETase and MHETase proteins. M, molecular marker; P, parent strain (Δ*pyrF*); Dp, Δ*petase* strain; Dm, Δ*mhetase* strain.

of both proteins in the Δ*pyrF* strain, whereas they were not detected in Δ*petase* and Δ*mhetase* transformants (Fig. 4). These results demonstrated that the transformants are Δ*petase* and Δ*mhetase* strains.

Characterization of Δ*petase* and Δ*mhetase* strains. To investigate the effects brought by the gene deletion, the Δ*pyrF* (parent), Δ*petase*, and Δ*mhetase* strains were grown in SV-uracil (Ura) medium with PET film, disodium terephthalate (TPA·2Na), or EG as a carbon source or without a carbon source (Fig. 5). The parent and disruptant strains displayed slight growth in the medium without a carbon source (Fig. 5A). Growth on medium without organic carbons might be due to the CO_2 fixation capacity of *I. sakaiensis*, predicted from the genomic information (13). Another possibility is that *I. sakaiensis* utilizes uracil as a carbon source, where uracil was supplemented to the minimum medium (SV medium) to grow Δ*pyrF* strains showing uracil auxotrophy. To test this hypothesis, the wild-type strain was grown in SV medium with and without uracil (10 μg/ml). The results showed that their growth levels were comparable (data not shown), indicating that uracil is not the major factor increasing *I. sakaiensis* growth. The cell yields of Δ*petase* and Δ*mhetase* strains cultured with PET were approximately 7-fold lower than that of the parent strain at 144 h and comparable to those cultured without a carbon source, respectively (Fig. 5A and B). Cultured with TPA·2Na, the cell yields of the disruptants were comparable to that of the parent, whose levels were significantly higher than those cultured without a carbon source (Fig. 5A and C). Cultured with EG, cell yields of the disruptants and parent strains were comparable, which were equivalent to those cultured without a carbon source (Fig. 5A and D). In addition, to evaluate the PET degradation capacity, the parent, Δ*petase*, and Δ*mhetase* strains were cultured in SV-Ura-PET medium for 10 days. The parent strain induced severe morphological change of the PET film surface (Fig. 6Aa) with significant weight loss of 6.9 mg (Fig. 6B), which corresponds to approximately 8% of the intact PET film. In contrast, in the Δ*petase* strain culture, no degradation traces (Fig. 6Ab) and weight change of PET film (Fig. 6B) were detected. Meanwhile, interestingly, the Δ*mhetase* strain degraded PET and only induced partial surface defects (Fig. 6Ac), resulting in a 1.4-mg weight loss of the PET film (Fig. 6B). Similar trends of the PET surface degradations were confirmed by eye (Fig. S5). These results indicate that *petase* and *mhetase* are essential for PET assimilation in *I. sakaiensis*.

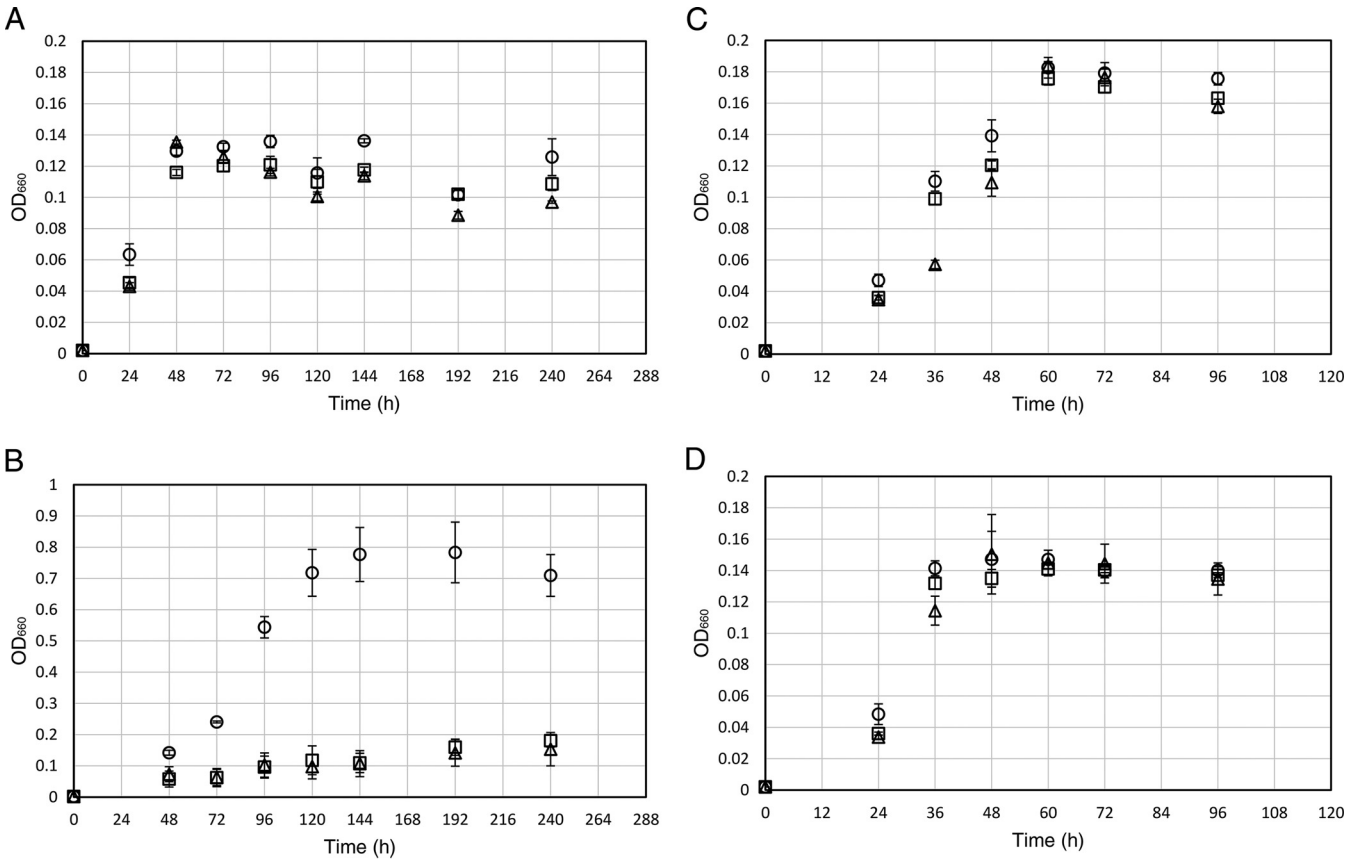

FIG 5 Growth of *I. sakaiensis* Δ*pyrF* and its mutant strains. The parent (Δ*pyrF*), Δ*petase*, and Δ*mhetase* strains were cultivated in SV-Ura (A), SV-Ura-PET (B), SV-Ura-TPA·2Na (C), and SV-Ura-EG (D). Circle, triangle, and square symbols indicate the parent, Δ*petase*, and Δ*mhetase* strains, respectively. The means ± standard deviations from three independent growth measurements are shown.

DISCUSSION

The ability of *I. sakaiensis* to degrade and assimilate PET has an applicable niche in the face of expanding environmental plastic pollution. In this study, we established a targeted gene disruption system of *I. sakaiensis* and identified the *in vivo* functions of PETase and MHETase using this system. This study reports the development of a gene manipulation system for *I. sakaiensis* that could serve to accelerate various *in vivo* studies on this bacterium, such as gene function analysis and metabolic engineering.

The positive selections using Tet and 5-FOA are completed on a nutrient-rich medium that is more convenient to prepare than the synthetic selection medium defined based on microbial auxotrophy. In a previous report, a genetic system in *Leptothrix discophora* SS1, belonging to *Betaproteobacteria*, was developed by constructing the Δ*pyrF* mutant by single-crossover homologous recombination, where *neo*, a marker gene used, remained on the genome (36). Therefore, gene disruption toward this Δ*pyrF* mutant allows only one gene but no additional genes using the same marker gene. In contrast, gene disruption in this study was developed by double-crossover homologous recombination, offering a resultant strain without marker genes containing *tetR′* and *pyrF* (Fig. 1B). Therefore, it can be applied for the disruption of multiple genes. This system would also be applicable for introducing mutations and exogenous genes into the *I. sakaiensis* genome using disruption vectors with a sequence of interest and the flanking sequences for homologous recombination.

In Δ*pyrF* strain construction (Fig. 1A), we also attempted unsuccessfully to pop out the plasmid including *sacB′* from the pop-in strain using sucrose rather than 5-FOA. *I. sakaiensis* might insufficiently express *sacB′*, owing to its inactive promoter in this

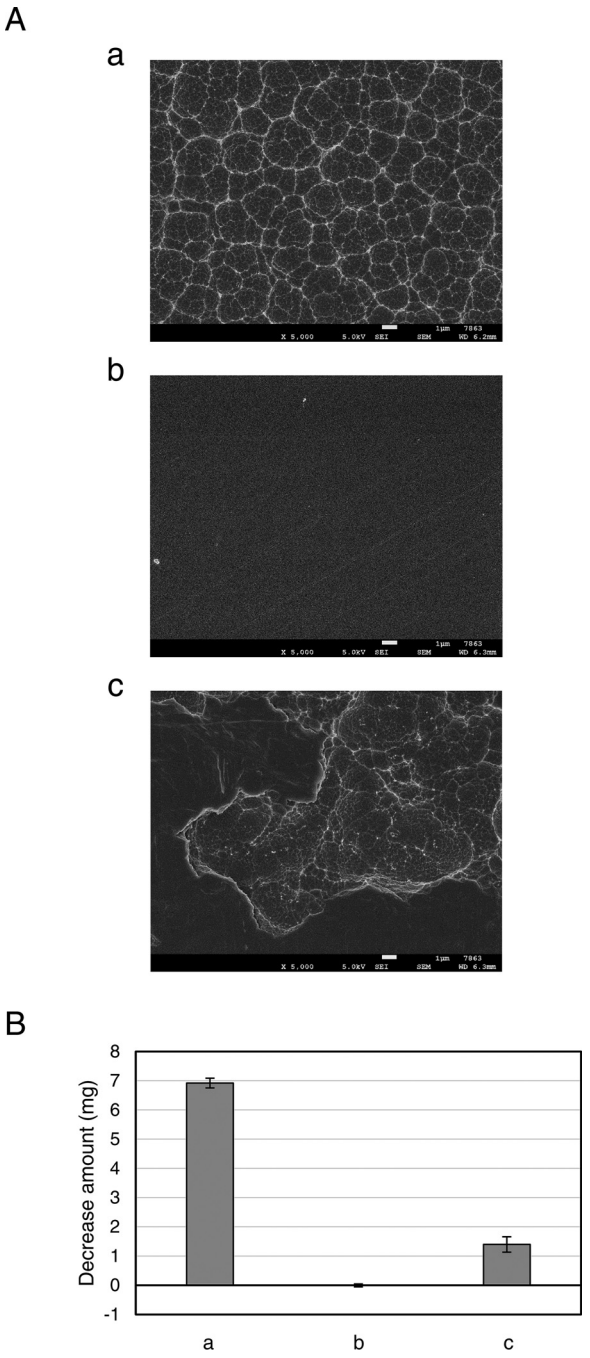

FIG 6 PET degradation by *I. sakaiensis* Δ*pyrF* and its mutant strains. The parent (Δ*pyrF*) (a), Δ*petase* (b), and Δ*mhetase* (c) strains were cultured with PET film in SV-Ura-PET at 30°C for 10 days. (A) SEM image of the degraded PET film surface. Scale bars represent 1 μm. Visual images of the corresponding samples are shown in Fig. S5. (B) Weight loss of PET films after cultivation relative to before cultivation. The means ± standard deviations are calculated from three independent experiments.

parent, fold the corresponding proteins incorrectly, and/or reduce the effect of increased sucrose or levan by a certain mechanism.

Based on the enzymatic activities of PETase and MHETase, we predicted the PET metabolic pathway in *I. sakaiensis*, where PET is hydrolyzed into MHET by PETase and the MHET is hydrolyzed into TPA and EG by MHETase (see Fig. S6 in the supplemental material) (8, 13). Compared to the Δ*pyrF* parent strain, both Δ*petase* and Δ*mhetase* strains showed dramatic reduction in growth on PET with no reduction on TPA (Fig. 5B

TABLE 1 Strains and plasmids used in this study

Strain/plasmid	Relevant feature(s)	Source or reference
Strains		
Ideonella sakaiensis		
201-F6	Wild-type strain	Lab stock (13)
Δ*pyrF*	Δ*pyrF*	This study
Δ*petase*	Δ*pyrF* Δ*petase*	This study
Δ*mhetase*	Δ*pyrF* Δ*mhetase*	This study
Escherichia coli		
DH5α	For cloning	TOYOBO
S17-1 (λpir)	For conjugation	NBRP (33)
Plasmids		
pK18*mobsacB*	Mobilizable vector in general (used for cloning in this study), Kan^r	NBRP (43)
pT18*mobsacB*	Mobilizable vector for gene disruption, Tet^r	Addgene (39)
pT′18*mobsacB*	pT18*mobsacB* derivative; *tetR* was replaced by *tetR*′, Tet^r	This study
pT′18*mobsacB*′	pT′18*mobsacB* derivative; *sacB* was replaced by *sacB*′, Tet^r	This study
pT′18*mobpyrF*	pT′*18mobsacB* derivative; *sacB* with its promoter was replaced by *I. sakaiensis*-derived sequence including *pyrF* and its promoter, Tet^r	This study
pT′*msB*′D*pyrF*	For *pyrF* disruption, pT′18*mobsacB*′ derivative, Tet^r	This study
pT′*mpF*D*petase*	For *petase* disruption, pT′18*mobpyrF* derivative, Tet^r	This study
pT′*mpF*D*mhetase*	For *mhetase* disruption, pT′18*mobpyrF* derivative, Tet^r	This study

and C). This demonstrates that PETase and MHETase are the primary *I. sakaiensis* enzymes carrying out hydrolytic activities toward PET and MHET, respectively. Together with the results that the Δ*petase* strain did not reduce the weight of PET film (Fig. 6B), we conclude that PETase is the sole enzyme that can hydrolyze PET in this bacterium. In contrast, the Δ*mhetase* strain induced weight loss of PET film, which corresponds to approximately 20% of that with the Δ*pyrF* strain (Fig. 6B). The ratio was proportional to their cell yields (Fig. 5B). These results indicate that MHETase is not essential for PET degradation but important for assimilating it.

I. sakaiensis strains, including the parent, Δ*petase*, and Δ*mhetase* strains, grew slightly on EG as a carbon source, but the cell yields were similar to those on no carbon source (Fig. 5A and D), indicating their incomplete EG metabolism. Given the prediction that MHETase locates in the periplasmic space (8, 13), *I. sakaiensis* may harbor the uptake system into the periplasm for MHET but not for EG. More importantly, growth levels of Δ*petase* and Δ*mhetase* strains on PET were similar to those cultivated without carbon source, indicating that PETase and MHETase are essential for assimilating PET. In addition, at earlier stages of cultivation, such as between 48 h and 72 h, their cell densities in a medium including PET were clearly lower than those without carbon source, which might be caused by the adherence of *I. sakaiensis* cells to the PET surface (13).

The gene manipulation technique developed in this study can be applied to the metabolic engineering and analysis of gene function in *I. sakaiensis*. We expect this genetic technique to lay the groundwork for PET recycling using *I. sakaiensis*.

MATERIALS AND METHODS

Strains, media, and culture conditions. Strains used in this study are summarized in Table 1. *E. coli* DH5α strain was used for cloning plasmids. *E. coli* S17-1 strain was used for transfer of plasmids into *I. sakaiensis* via conjugation. *E. coli* cells were cultivated in lysogeny broth (LB) medium supplemented with appropriate antibiotics at 37°C. *I. sakaiensis* cells were cultivated as described previously (13) with slight modifications. The cultivation was performed at 30°C in either 5 ml liquid medium in a test tube (diameter, 18 by 180 mm) with shaking at 300 strokes/min or on a 1.5% agar plate. The media used in this study are the following: nutrient-rich medium NBRC 802 (NBRC802) and sodium carbonate-vitamin (SV) medium (yeast extract-depleted from YSV medium) containing 0.2 g/liter sodium hydrogen carbonate, 1 g/liter ammonium sulfate, 0.1 g/liter calcium carbonate, 0.01 g/liter iron(II) sulfate heptahydrate, trace elements [10 mg/liter magnesium sulfate heptahydrate, 1 mg/liter copper(II) sulfate pentahydrate, 1 mg/liter manganese(II) sulfate pentahydrate, and 1 mg/liter zinc sulfate heptahydrate], and vitamin mix (2.5 mg/liter thiamine hydrochloride, 0.05 mg/liter biotin, and 0.5 mg/liter vitamin B12) in 10 mM Na_2HPO_4-NaH_2PO_4 (pH 7.4).

PET film with a crystallinity of 2.4%, determined by differential scanning calorimetry, disodium terephthalate (TPA·2Na), EG, or D-(+)-maltose monohydrate (Mal·H_2O) was added to the SV medium as a carbon source. Tetracycline hydrochloride (Tet·HCl), kanamycin sulfate (Kan·nH_2SO_4), uracil (Ura), and 5-fluoroorotic acid monohydrate (5-FOA·H_2O) were supplemented to the media when necessary.

Plasmid construction. Plasmids and primers used in this study are summarized in Table 1 and Table S1 in the supplemental material, respectively. DNA sequences of *tetR* and *sacB* in pT18*mobsacB* (39) were codon optimized for expression in *I. sakaiensis* based on the codon usage database of *Ideonella dechloratans* by Kazusa DNA Research Institute (https://www.kazusa.or.jp/codon/) (Fig. S1) and synthesized by Integrated DNA Technologies (Coralville, IA), resulting in *tetR*′ and *sacB*′. Primers for inverse-PCR toward pT18*mobsacB* were constructed so that the regions to be exchanged were removed. The inverse PCR fragment was fused with *tetR*′ and *sacB*′ using and In-Fusion HD cloning kit (TaKaRa Bio, Shiga, Japan), resulting in pT′18*mobsacB* and pT′18*mobsacB*′, respectively. The promoter region of *pyrF* was predicted with the online software BPROM (prediction of bacterial promoters; http://www.softberry.com/berry.phtml?topic=bprom&group=programs&subgroup=gfindb) (40). *sacB* and its promoter region in pT′18*mobsacB* were removed by inverse PCR and fused with *pyrF* with its promoter region amplified from *I. sakaiensis* genomic DNA (Fig. S3), resulting in pT′18*mobpyrF*. For the *pyrF* disruption vector, the 5′ 709 bp and 3′ 770 bp of *pyrF* on the *I. sakaiensis* genome (shown in Fig. S3) were amplified. These two fragments were fused by overlap extension PCR using dpyrF1_IF-F/dpyrF2_IF-R primers and inserted into the SmaI site in pT′18*mobsacB*′ by In-Fusion cloning, producing pT′*msB*′D*pyrF*. For the *petase* disruption vector, a DNA fragment including *petase* and its flanking regions (5′ 750 bp and 3′ 750 bp) was amplified from the genomic DNA using dpetase_IF-F/dpetase_IF-R primers. The fragment was inserted into the SmaI site of pK18*mobsacB* plasmid by In-Fusion cloning. *petase* in the obtained plasmid was removed by inverse PCR using 5′-phosphorylated primers of inv-dpetase-F and inv-dpetase-R, followed by self-ligation to cyclize the vector. The 1,500-bp region including the 5′ 750 bp and 3′ 750 bp was amplified with dpetase_IF-F/dpetase_IF-R and inserted into the SmaI site of pT′18*mobpyrF* plasmid through In-Fusion cloning, giving pT′*mpF*D*petase*. For the *mhetase* disruption vector, the 5′ 648 bp and 3′ 641 bp of *mhetase* on the genome were amplified. The fragments were fused by overlap extension PCR using dmhetase1_IF-F/dmhetase2_IF-R primers and inserted into the SmaI site in pT′18*mobpyrF*, producing pT′*mpF*D*mhetase*. The integrity of the plasmids was confirmed by DNA sequencing. The genomic DNA of *I. sakaiensis* was extracted by using a Wizard genomic DNA purification kit from Promega (Madison, WI).

Construction of Δ*pyrF*, Δ*petase*, and Δ*mhetase* strains. Conjugation from *E. coli* S17-1 (donor) to *I. sakaiensis* (recipient) was performed as previously described (41, 42), with modifications. *I. sakaiensis* (wild-type or Δ*pyrF* strain) was cultivated in NBRC802 for 2 days. *E. coli* S17-1 transformant with the disruption vector (pT′*msB*′D*pyrF*, pT′*mpF*D*petase*, or pT′*mpF*D*mhetase*) was cultivated in NBRC802-Tet·HCl (10 μg/ml) at 30°C overnight. When the absorbance at 660 nm of both cultures exceeded 1.0, cells were harvested from 2 ml of *I. sakaiensis* culture and 1 ml of *E. coli* S17-1 culture by centrifugation (5,000 × *g*, 5 min) and suspended with 500 μl of NBRC802. They were thoroughly mixed, harvested, and resuspended with 100 μl of NBRC802. The mixture was dropped onto a nitrocellulose membrane (Merck Millipore, Burlington, MA) on an NBRC802 agar plate and incubated at 30°C for 2 days. The cells on the membrane were suspended with NBRC802 and plated onto an NBRC802-Tet·HCl (5 μg/ml or 10 μg/ml)-Kan·nH_2SO_4 (20 μg/ml) agar. Colonies were evaluated by PCR using M13F/dpyrF_out-f and M13R/dpyrF_out-r (for Δ*pyrF*), M13F/dPETase_out-f and M13R/dPETase_out-r (for Δ*petase*), or M13F/dMHETase_out-f and M13R/dMHETase_out-r (for Δ*mhetase*) to select the pop-in strains. The pop-in strains were cultivated in NBRC802-Tet·HCl (10 μg/ml), harvested, washed with NBRC802, and plated onto SV-Mal·H_2O (1 mg/ml)-Ura (10 μg/ml)-5-FOA·H_2O (55 μg/ml)-Kan·nH_2SO_4 (10 μg/ml) agar or NBRC802-Ura (10 μg/ml)-5-FOA·H_2O (55 μg/ml)-Kan·nH_2SO_4 (10 μg/ml) agar. PCR analysis toward the colonies using dpyrF_out-f/dpyrF_out-r and dpyrF_in-f/dpyrF_in-r (for Δ*pyrF*), dPETase_out-f/dPETase_out-r and dPETase_in-f/dPETase_in-r (for Δ*petase*), or dMHETase_out-f/dMHETase_out-r and dMHETase_in-f/dMHETase_in-r (for Δ*mhetase*) was performed to select the disruption strains. The integrity of the homologous regions of disruption strains was confirmed by DNA sequencing.

Uracil auxotrophy and 5-FOA resistance of the Δ*pyrF* strain. The wild-type and Δ*pyrF* strains were cultivated in NBRC802 at 30°C for 2 days and harvested by centrifugation (5,000 × *g*, 5 min). The cells were suspended using SV without vitamin mix to adjust the absorbance at 660 nm to 0.1. Ten microliters of the suspension was dropped onto agar plates of SV-Mal·H_2O (1 mg/ml), SV-Mal·H_2O (1 mg/ml)-Ura (10 μg/ml), and SV-Mal·H_2O (1 mg/ml)-Ura (10 μg/ml)-5-FOA·H_2O (55 μg/ml) and streaked with an inoculating needle. The plates were incubated at 30°C for 5 days.

Western blot analysis. The Δ*pyrF* (parent), Δ*petase*, and Δ*mhetase* strains were cultivated in SV-TPA·2Na (1 mM)-Ura (10 μg/ml) at 30°C for 3 days. For protein denaturation, the culture fluid was vortexed in 3% (wt/vol) Triton X-100 and incubated at room temperature for 10 min. The samples were subjected to SDS-PAGE using 12.5% acrylamide gel followed by blotting to a polyvinylidene difluoride (PVDF) membrane (Clear Blot Membrane-P plus from ATTO, Tokyo, Japan). The primary antibodies were created as follows. PETase and MHETase were expressed as previously described (13) and purified through nickel-affinity chromatography under denaturing conditions using 6 M guanidine-HCl. Rabbit and guinea pig were immunized with purified PETase and MHETase, respectively, at Eurofins Genomics (Tokyo, Japan). Polyclonal antibodies were purified from antiserum by utilizing their affinities with the corresponding antigens. As secondary antibodies, goat anti-rabbit IgG conjugated with horseradish peroxidase (HRP) (Invitrogen [Thermo Fisher Scientific], Waltham, MA) and goat anti-guinea pig IgG HRP conjugate (Invitrogen [Thermo Fisher Scientific]) were used. After antibody labeling, the PVDF membrane was reacted with Chemi-Lumi One Super (Nacalai Tesque, Kyoto, Japan), and the band signals were visualized using ImageQuant LAS 500 (GE Healthcare, Chicago, IL).

Growth of mutant strains. The parent, the Δ*petase*, and the Δ*mhetase* strains were cultivated in NBRC802 for 2 days until their absorbance at 660 nm exceeded 1.0. Cells were harvested and suspended using SV without vitamin mix. The suspension was inoculated to SV-Ura (10 μg/ml) with or without PET film (ca. 85 mg, 20 by 15 by 0.2 mm^3), 1 mM TPA·2Na, or 1 mM EG as a carbon source to adjust the absorbance at 660 nm to 0.002 and shaken at 300 strokes/min at 30°C. The growth of three independent cultures was monitored with the absorbance at 660 nm. After cultivation, PET films were washed with 10% (wt/vol) SDS, distilled water, 5% SDS, distilled water, 1% SDS, distilled water (2 times), and 70% ethanol (3 times), in that order, with shaking. The air-dried PET film was weighed, and the weight reduction was calculated. The specimen was coated with osmium tetroxide using osmium plasma coater OPC-80 (Nippon Laser & Electronics Lab, Nagoya, Japan) and observed using a JSM-7500F (JEOL, Tokyo, Japan) at Hanaichi UltraStructure Research Institute (Okazaki, Japan).

Data availability. All data generated during this study are included in this published article and the supplemental material files.

SUPPLEMENTAL MATERIAL

Supplemental material is available online only.

SUPPLEMENTAL FILE 1, PDF file, 0.8 MB.

ACKNOWLEDGMENTS

We thank Kohei Oda for the kind gift of *I. sakaiensis*. We are grateful to Tetsu Shimizu, Kazumi Hiraga, and Masayuki Inui for assistance with the conjugation technique. We also thank Kai Uchizato for research assistance. *E. coli* S17-1 and pK18*mobsacB* were provided by the National BioResource Project (NBRP; Japan).

This work was supported by JSPS KAKENHI (19K15735 to S.-I.H., 17H03794 and 18K19177 to S.Y.) and the Leading Initiative for Excellent Young Researchers (LEADER) program by MEXT (to S.Y.).

REFERENCES

1. Geyer R, Jambeck JR, Law KL. 2017. Production, use, and fate of all plastics ever made. Sci Adv 3:e1700782. https://doi.org/10.1126/sciadv.1700782.
2. Jambeck JR, Geyer R, Wilcox C, Siegler TR, Perryman M, Andrady A, Narayan R, Law KL. 2015. Marine pollution. Plastic waste inputs from land into the ocean. Science 347:768–771. https://doi.org/10.1126/science.1260352.
3. Lebreton LCM, van der Zwet J, Damsteeg JW, Slat B, Andrady A, Reisser J. 2017. River plastic emissions to the world's oceans. Nat Commun 8:15611. https://doi.org/10.1038/ncomms15611.
4. Talsness CE, Andrade AJ, Kuriyama SN, Taylor JA, Vom Saal FS. 2009. Components of plastic: experimental studies in animals and relevance for human health. Philos Trans R Soc Lond B Biol Sci 364:2079–2096. https://doi.org/10.1098/rstb.2008.0281.
5. Thompson RC, Moore CJ, Vom Saal FS, Swan SH. 2009. Plastics, the environment and human health: current consensus and future trends. Philos Trans R Soc Lond B Biol Sci 364:2153–2166. https://doi.org/10.1098/rstb.2009.0053.
6. Tokiwa Y, Calabia BP, Ugwu CU, Aiba S. 2009. Biodegradability of plastics. Int J Mol Sci 10:3722–3742. https://doi.org/10.3390/ijms10093722.
7. Webb HK, Arnott J, Crawford RJ, Ivanova EP. 2012. Plastic degradation and its environmental implications with special reference to poly (ethylene terephthalate). Polymers 5:1–18. https://doi.org/10.3390/polym5010001.
8. Taniguchi I, Yoshida S, Hiraga K, Miyamoto K, Kimura Y, Oda K. 2019. Biodegradation of PET: current status and application aspects. ACS Catal 9:4089–4105. https://doi.org/10.1021/acscatal.8b05171.
9. Sinha V, Patel MR, Patel JV. 2010. Pet waste management by chemical recycling: a review. J Polym Environ 18:8–25. https://doi.org/10.1007/s10924-008-0106-7.
10. Geyer B, Lorenz G, Kandelbauer A. 2016. Recycling of poly (ethylene terephthalate)-A review focusing on chemical methods. Express Polym Lett 10:559–586. https://doi.org/10.3144/expresspolymlett.2016.53.
11. Müller R-J, Schrader H, Profe J, Dresler K, Deckwer W-D. 2005. Enzymatic degradation of poly(ethylene terephthalate): rapid hydrolyse using a hydrolase from *T. fusca*. Macromol Rapid Commun 26:1400–1405. https://doi.org/10.1002/marc.200500410.
12. Kawai F, Kawabata T, Oda M. 2019. Current knowledge on enzymatic PET degradation and its possible application to waste stream management and other fields. Appl Microbiol Biotechnol 103:4253–4268. https://doi.org/10.1007/s00253-019-09717-y.
13. Yoshida S, Hiraga K, Takehana T, Taniguchi I, Yamaji H, Maeda Y, Toyohara K, Miyamoto K, Kimura Y, Oda K. 2016. A bacterium that degrades and assimilates poly(ethylene terephthalate). Science 351:1196–1199. https://doi.org/10.1126/science.aad6359.
14. Hiraga K, Taniguchi I, Yoshida S, Kimura Y, Oda K. 2020. Biodegradation of waste PET. EMBO Rep 21:e49826. https://doi.org/10.15252/embr.201949826.
15. Tanasupawat S, Takehana T, Yoshida S, Hiraga K, Oda K. 2016. *Ideonella sakaiensis* sp. nov., isolated from a microbial consortium that degrades poly(ethylene terephthalate). Int J Syst Evol Microbiol 66:2813–2818. https://doi.org/10.1099/ijsem.0.001058.
16. Han X, Liu W, Huang J-W, Ma J, Zheng Y, Ko T-P, Xu L, Cheng Y-S, Chen C-C, Guo R-T. 2017. Structural insight into catalytic mechanism of PET hydrolase. Nat Commun 8:2106. https://doi.org/10.1038/s41467-017-02255-z.
17. Austin HP, Allen MD, Donohoe BS, Rorrer NA, Kearns FL, Silveira RL, Pollard BC, Dominick G, Duman R, El Omari K, Mykhaylyk V, Wagner A, Michener WE, Amore A, Skaf MS, Crowley MF, Thorne AW, Johnson CW, Woodcock HL, McGeehan JE, Beckham GT. 2018. Characterization and engineering of a plastic-degrading aromatic polyesterase. Proc Natl Acad Sci U S A 115:E4350–E4357. https://doi.org/10.1073/pnas.1718804115.
18. Chen CC, Han X, Ko TP, Liu W, Guo RT. 2018. Structural studies reveal the molecular mechanism of PETase. FEBS J 285:3717–3723. https://doi.org/10.1111/febs.14612.
19. Fecker T, Galaz-Davison P, Engelberger F, Narui Y, Sotomayor M, Parra LP, Ramírez-Sarmiento CA. 2018. Active site flexibility as a hallmark for efficient PET degradation by *I. sakaiensis* PETase. Biophys J 114:1302–1312. https://doi.org/10.1016/j.bpj.2018.02.005.
20. Joo S, Cho IJ, Seo H, Son HF, Sagong HY, Shin TJ, Choi SY, Lee SY, Kim KJ. 2018. Structural insight into molecular mechanism of poly(ethylene terephthalate) degradation. Nat Commun 9:382. https://doi.org/10.1038/s41467-018-02881-1.
21. Liu B, He L, Wang L, Li T, Li C, Liu H, Luo Y, Bao R. 2018. Protein crystallography and site-direct mutagenesis analysis of the poly(ethylene terephthalate) hydrolase PETase from *Ideonella sakaiensis*. Chembiochem 19:1471–1475. https://doi.org/10.1002/cbic.201800097.
22. Palm GJ, Reisky L, Böttcher D, Müller H, Michels EAP, Walczak MC, Berndt L, Weiss MS, Bornscheuer UT, Weber G. 2019. Structure of the plastic-degrading *Ideonella sakaiensis* MHETase bound to a substrate. Nat Commun 10:1717. https://doi.org/10.1038/s41467-019-09326-3.

23. Knott BC, Erickson E, Allen MD, Gado JE, Graham R, Kearns FL, Pardo I, Topuzlu E, Anderson JJ, Austin HP, Dominick G, Johnson CW, Rorrer NA, Szostkiewicz CJ, Copié V, Payne CM, Woodcock HL, Donohoe BS, Beckham GT, McGeehan JE. 2020. Characterization and engineering of a two-enzyme system for plastics depolymerization. Proc Natl Acad Sci U S A https://doi.org/10.1073/pnas.2006753117.
24. Ma Y, Yao M, Li B, Ding M, He B, Chen S, Zhou X, Yuan Y. 2018. Enhanced poly (ethylene terephthalate) hydrolase activity by protein engineering. Engineering 4:888–893. https://doi.org/10.1016/j.eng.2018.09.007.
25. Cui Y, Chen Y, Liu X, Dong S, Ye T, Qiao Y, Han J, Li C, Han X, Liu W, Chen Q, Du W, Tang S, Xiang H, Liu H, Wu B. 2019. Computational redesign of PETase for plastic biodegradation by GRAPE strategy. bioRxiv https://doi.org/10.1101/787069.
26. Son HF, Cho IJ, Joo S, Seo H, Sagong H-Y, Choi SY, Lee SY, Kim K-J. 2019. Rational protein engineering of thermo-stable PETase from *Ideonella sakaiensis* for highly efficient PET degradation. ACS Catal 9:3519–3526. https://doi.org/10.1021/acscatal.9b00568.
27. Son HF, Joo S, Seo H, Sagong H-Y, Lee SH, Hong H, Kim K-J. 2020. Structural bioinformatics-based protein engineering of thermo-stable PETase from *Ideonella sakaiensis*. Enzyme Microb Technol 141:109656. https://doi.org/10.1016/j.enzmictec.2020.109656.
28. Furukawa M, Kawakami N, Oda K, Miyamoto K. 2018. Acceleration of enzymatic degradation of poly(ethylene terephthalate) by surface coating with anionic surfactants. ChemSusChem 11:4018–4025. https://doi.org/10.1002/cssc.201802096.
29. Huang X, Cao L, Qin Z, Li S, Kong W, Liu Y. 2018. Tat-independent secretion of polyethylene terephthalate hydrolase PETase in *Bacillus subtilis* 168 mediated by its native signal peptide. J Agric Food Chem 66:13217–13227. https://doi.org/10.1021/acs.jafc.8b05038.
30. Moog D, Schmitt J, Senger J, Zarzycki J, Rexer KH, Linne U, Erb T, Maier UG. 2019. Using a marine microalga as a chassis for polyethylene terephthalate (PET) degradation. Microb Cell Fact 18:171. https://doi.org/10.1186/s12934-019-1220-z.
31. Seo H, Kim S, Son HF, Sagong HY, Joo S, Kim KJ. 2019. Production of extracellular PETase from *Ideonella sakaiensis* using sec-dependent signal peptides in *E. coli*. Biochem Biophys Res Commun 508:250–255. https://doi.org/10.1016/j.bbrc.2018.11.087.
32. Kim JW, Park SB, Tran QG, Cho DH, Choi DY, Lee YJ, Kim HS. 2020. Functional expression of polyethylene terephthalate-degrading enzyme (PETase) in green microalgae. Microb Cell Fact 19:97. https://doi.org/10.1186/s12934-020-01355-8.
33. Simon R, Priefer U, Pühler A. 1983. A broad host range mobilization system for *in vivo* genetic engineering: transposon mutagenesis in Gram negative bacteria. Nat Biotechnol 1:784–791. https://doi.org/10.1038/nbt1183-784.
34. Boeke JD, LaCroute F, Fink GR. 1984. A positive selection for mutants lacking orotidine-5′-phosphate decarboxylase activity in yeast: 5-fluoro-orotic acid resistance. Mol Gen Genet 197:345–346. https://doi.org/10.1007/BF00330984.
35. Sato T, Fukui T, Atomi H, Imanaka T. 2003. Targeted gene disruption by homologous recombination in the hyperthermophilic archaeon *Thermococcus kodakaraensis* KOD1. J Bacteriol 185:210–220. https://doi.org/10.1128/JB.185.1.210-220.2003.
36. Bocioaga D, El Gheriany IA, Lion LW, Ghiorse WC, Shuler ML, Hay AG. 2014. Development of a genetic system for a model manganese-oxidizing proteobacterium, *Leptothrix discophora* SS1. Microbiology 160:2396–2405. https://doi.org/10.1099/mic.0.079459-0.
37. Gay P, Le Coq D, Steinmetz M, Berkelman T, Kado CI. 1985. Positive selection procedure for entrapment of insertion sequence elements in gram-negative bacteria. J Bacteriol 164:918–921. https://doi.org/10.1128/jb.164.2.918-921.1985.
38. Reyrat J-M, Pelicic V, Gicquel B, Rappuoli R. 1998. Counterselectable markers: untapped tools for bacterial genetics and pathogenesis. Infect Immun 66:4011–4017. https://doi.org/10.1128/IAI.66.9.4011-4017.1998.
39. Wei HL, Chakravarthy S, Worley JN, Collmer A. 2013. Consequences of flagellin export through the type III secretion system of *Pseudomonas syringae* reveal a major difference in the innate immune systems of mammals and the model plant *Nicotiana benthamiana*. Cell Microbiol 15:601–618. https://doi.org/10.1111/cmi.12059.
40. Solovyev V, Salamov A. 2011. Automatic annotation of microbial genomes and metagenomic sequences, p 61–78. *In* Li RW (ed), Metagenomics and its applications in agriculture, biomedicine and environmental studies. Nova Science Publishers, Hauppauge, NY.
41. Koehler TM, Thorne CB. 1987. *Bacillus subtilis* (*natto*) plasmid pLS20 mediates interspecies plasmid transfer. J Bacteriol 169:5271–5278. https://doi.org/10.1128/jb.169.11.5271-5278.1987.
42. Shimizu T, Teramoto H, Inui M. 2019. Introduction of glyoxylate bypass increases hydrogen gas yield from acetate and L-glutamate in *Rhodobacter sphaeroides*. Appl Environ Microbiol 85:e01873-18. https://doi.org/10.1128/AEM.01873-18.
43. Schäfer A, Tauch A, Jäger W, Kalinowski J, Thierbach G, Pühler A. 1994. Small mobilizable multi-purpose cloning vectors derived from the *Escherichia coli* plasmids pK18 and pK19: selection of defined deletions in the chromosome of *Corynebacterium glutamicum*. Gene 145:69–73. https://doi.org/10.1016/0378-1119(94)90324-7.